STRESSES IN A TORISPHERICAL HEAD OF A PRESSURE VESSEL BY PHOTOELASTIC COATING METHOD

by

LASZLO IMRE SZEKESSY

Dipl. Mech. Eng.

Technical University Budapest, 1950.

A THESIS SUBMITTED IN PARTIAL FULFILMENT OF

THE REQUIREMENTS FOR THE DEGREE OF

MASTER OF APPLIED SCIENCE

in the Department

of

MECHANICAL ENGINEERING

We accept this thesis as conforming to the required standard

THE UNIVERSITY OF BRITISH COLUMBIA
October, 1961

In presenting this thesis in partial fulfilment of the requirements for an advanced degree at the University of British Columbia, I agree that the Library shall make it freely available for reference and study. I further agree that permission for extensive copying of this thesis for scholarly purposes may be granted by the Head of my Department or by his representatives. It is understood that copying or publication of this thesis for financial gain shall not be allowed without my written permission.

Department of Mechanical Engineering

The University of British Columbia,
Vancouver 8, Canada.

Date Vancouver, October 1. 1961

Abstract.

The use of the photoelastic coating method in determining the stresses in the torispherical head of a pressure vessel was investigated.

It was found that the method is valuable to obtain the distribution, direction, and magnitude of stresses on the surface of any structure.

The results obtained with the method showed close agreement with the theoretical investigations. The maximum stresses in a torispherical head of a pressure vessel occur in the torus. The same conclusion was drawn from the results obtained with the method. It also revealed, that these stresses were compressive on the outer surface.

The mobility of the instruments, the relatively simple way of coating the surface of the structure are other features of the method.

ACKNOWLEDGMENT

The author wishes to express his gratitude to Professor W. O. Richmond, Head of the Department of Mechanical Engineering, for the guidance in completing his work, for making the instruments and laboratories freely available and for the help in obtaining financial assistance.

TABLE OF CONTENTS

LIST OF TABLES

LIST OF FIGURES

List of Symbols Used.

E	(lb/in^2)	Modulus of Elasticity
ν		Poisson's ratio
t	(in)	Thickness
C	(in^2/lb)	Stress optical coefficient
C_1, C_2		Correction factors
$K = \frac{CE_p}{1 + \nu_p}$		Optical strain sensitivity factor of plastic
δ	(in)	Relative retardation of polarized light
ϵ_1; ϵ_2	(in/in)	Principal strains
σ_1; σ_2	(lb/in^2)	Principal stresses
σ	(lb/in^2)	Normal stress
τ	(lb/in^2)	Shear stress
R	(in)	Radius of head or cylinder
r	(in)	Radius of the knuckle
p	(psig)	Pressure acting in the pressure vessel
M	(in/lb)	Bending moment
L	(in)	Distance
F	(lb)	Load
I	(in^4)	Moment of inertia

f		Fringe value of the plastic used
λ	(in)	Wave length of light
θ	(degr.)	Angle of incidence of light
ϕ	(degr.)	Angle between a normal to the surface of the shell and the shell axis
α	(degr.)	Angle between a normal drawn to the shell axis from the junction of the cylinder and head and a line from a point on the surface of the head.
β	(degr.)	Compensator reading on the large field polariscope.
m		The difference of readings taken at a point using the oblique incidence polariscope when the structure is loaded and unloaded.

Subscripts.

c = cylinder

p = plastic

n = normal

o = oblique

w = metal, workpiece

Introduction.

Stress analysis by photoelasticity depends upon the property of temporary double refraction or artificial birefringence possessed by certain transparent materials. This birefringence is proportional to stress and hence it is possible to deduce the stress from the observation of the optical properties. Ordinary methods of photoelastic stress analysis use a plastic model of the structure under analysis. A newer technique uses a coating of transparent photoelastic material cemented to the metal part under investigation so that the photoelastic effect observed is a function of the strain on the surface of the structure. In this investigation the coating method is used in a study of the stress distribution in a toroidal shell.

The use of birefringent coating in photoelastic investigation was initiated by Mesnager (France) in 1930 (1), who used a birefringent layer of glass. There was no satisfactory bond to the structure investigated and practical results were not produced at that time. Several attempts to develop the coating method by Mabboux (France) 1932 (2), and Oppel (Germany) 1937 (3), were unsuccessful for practical use, because the coating material still had low sensitivity, and the bonding was insufficient.

In the United States of America D'Agostino, Drucker,

Lin, and Mylonas performed extensive studies of the behaviour of birefringent coatings (4,5) and developed it as a practical tool for stress analysis. They presented the results of their work at the convention of IUTAM in Brussels in 1954.

Practical results achieved on the industrial level in France were published by Zandman (5,6). The coating method was used on various structural materials in both elastic and plastic ranges of deformation. The coating material proved to be stable in time and temperature. The bond was effective thus providing the necessary traction between the plastic and the metal.

Description of the Photoelastic Coating Method.

The structural part to be analysed is coated with a layer of birefringent material cemented to the surface so that the strains are transmitted to the plastic (7,8). A reflecting surface is provided between the metal and the plastic. Birefringence due to strain is observed by a reflection polariscope so that the light ray passes twice through the plastic layer. Because of this, the basic law of photoelasticity expressing the relative retardation between the ordinary and extraordinary ray and the difference between the principal stresses is (9,10)

$$\delta_n = C\ (\sigma_1 - \sigma_2)\ 2\ t$$

where δ = is the relative retardation,

C = is the stress optical coefficient

σ_1 and σ_2 are principal stresses

t = is the thickness of the plastic layer

When the part is strained, black and coloured fringes are visible through the analyzer plate of the polariscope using white light. If the polarizing axes of the polarizer and analyzer plates are crossed, the black fringes represent isoclinics. Isoclinics are the loci of points where the directions of the principal stresses are constant and the same as the directions of the polarizing axes of the polariscope.

The directions of the principal stresses therefore can be determined at every point because the crossed analyzer and polarizer plates can be rotated simultaneously. Knowing the directions of the principal stresses at every point it is possible to plot the stress trajectories (isostatics) (9,10).

When the quantitative evaluation of the fringes is considered the isoclinics should be eliminated. This is achieved by inserting two quarter wave plates in the path of the polarised light. The quarter wave plates are made of birefringent material of such a thickness that the retardation between the ordinary and extraordinary rays is one quarter of the wave length of the monochromatic light used.

One quarter wave plate is placed between the polarizer plate and the plastic, the other between the plastic coat and the analyzer plate (Fig.1.). The two quarter plates convert the plane polarized light to circular polarized light. In the case of white light this is not quite true since the light becomes elliptically polarized, but the difference is very small and has little effect on the scale of interference colours (12).

The fringes seen in the circular polarized white light are coloured. If the incidence of the circular polarized light is normal, these coloured fringes are the loci of points where the difference of the principal stresses is

constant. A black fringe in the circular polarized light indicates that at those points the difference of the principal stresses is zero.

As shown in Appendix I, by determining the retardations at points on the plastic the stresses in the structure are given by the equation

$$(\sigma_1 - \sigma_2)_w = \frac{E_w}{1 + \nu_w} \frac{\delta_n}{2\ t\ K}$$

where $K = \frac{CE_p}{1 + \nu_p}$ is the optical strain sensitivity factor of the plastic. It is obtained by calibration.

E = modulus of elasticity

ν = Poisson's ratio

δ = relative retardation

The half of the principal stress difference so defined, gives the maximum shear stress, as known from the theory of elasticity (13).

$$\tau_{max} = \frac{1}{2} (\sigma_1 - \sigma_2)$$

Therefore the coloured fringes sometimes are called the constant shear stress lines.

In particular state of stress, if the direction of the principal stresses and their difference determined by the

fringes is known, the individual principal stresses may be determined mathematically. Often the stresses are sought along free boundaries such as in the case of a hole or a notch where the stress normal to the boundary is zero, and the fringe value gives the tangential stress directly. When this is not the case additional photoelastic measurements are necessary.

If the polarized light has an oblique angle of incidence the fringes obtained will represent the difference of the secondary principal stresses (9). Secondary principal stresses are defined as the principal stresses resulting from the stress components lying in a plane normal to the given direction. By choosing the plane of incident and reflected light properly it is always possible to include one of the principal stresses into the difference of the secondary principal stresses. Having this additional reading with the normal reading, (or two oblique readings) the individual principal stresses can be calculated (14).

For practical reasons the angle of oblique incidence is chosen as 45° resulting in great simplifications in the expressions for the individual principal stresses. The instrument used is again a reflection polariscope, the polarizer and analyzer plates being set with their polarizing axes crossed and at 45° to the plane of the incident and reflected rays (Fig.2). The 45° setting of the polarizing axes was

required by the quartz wedge compensator. This compensator is situated ahead of the analyzer plate in the reflected light path. The plane of incident and reflected light should always coincide with one of the principal stress directions. The compensator value so obtained refers to the principal stress perpendicular to the plane of incident and reflected light. The magnitude of the principal stresses is given by the equations as derived in Appendix I.

$$(\sigma_1)_w = 2.36 \times 10^{-7} \frac{E_w}{t K} \left(m_1 + \frac{m_2}{2} \right)$$

$$(\sigma_2)_w = 2.36 \times 10^{-7} \frac{E_w}{t K} \left(m_2 + \frac{m_1}{2} \right)$$

where m_1 and m_2 are the compensator reading changes occurring due to load (15). The oblique incidence readings are taken always after all the normal readings are completed and the directions of the principal stresses are known.

There are different ways to evaluate the retardation or fringe value and hence the magnitude of principal stresses. The first, and least accurate, is the comparison of the fringe colour to a standard colour scale which is related to strain through calibration. If a black fringe is present, one can count the number of successive "tint of passage" fringes. The tint of passage is the colour occurring at the transition from

red to blue. This dull purple colour is very sensitive to small changes in the difference of the principal stresses but gives accurate stress readings only when the point under investigation lies on a tint of passage. Often the stress is not high enough to produce strains corresponding to one fringe or the point under investigation lies between successive fringes. In this case an optical compensator should be used, which produces a tint of passage at any point of the birefringent plastic, at any value of strain. The most accurate method of defining fractions of fringes is to use photometers.

The method of application of birefringent layers depends on the shape of the structure and also on the accuracy required (16). For plane surfaces, plastic sheets are available in various thickness. These sheets are bonded to the surface by means of an adhesive. To provide a reflective surface at the interface of the structure and coating, the adhesive usually is mixed with aluminum powder. In case the surface of the metal is ground this is not necessary because the diffuse reflection provided by the surface is satisfactory for the observation of the fringes. When a high degree of accuracy is not required the plastic can be applied by brushing liquid plastic on the surface of the structure, and polymerizing it by heat applied to the coated area (17). For quantitative analysis the thickness of the coat must be also

measured at the point under investigation. When the surface is complicated it is best to use contoured sheets. For contoured sheets the plastic is cast on a glass plate and taken from the glass when partially polymerized (18). In this state the plastic sheet is easily formed without introducing initial birefringence. The sheet is moulded over the required surface, and is left on the surface until the polymerization is completed (generally 24 hours).When hard, the moulded plastic is bonded to the surface of the structure with a cement, as for the sheet plastic. When casting, a strip is set aside for calibration purposes. It is bonded to a test bar in which the surface strains may be obtained by calculation. Measuring the retardation in the plastic, the strain optical coefficient of the plastic can be determined, as shown in Appendix III, using the equation

$$K = \frac{\delta}{2\,t\,(\epsilon_1 - \epsilon_2)}$$

For high stress gradients or sharp curvatures, a polarizing microscope is used (Fig.3). This consists of an objective, a pair of crossed Nicols, one compensator wedge and one ocular. The light source may be either attached to the tube, or to a separate stand. The total magnification is about twenty times.

The accuracy of the measurements taken with the polari-

scope is defined by the accuracy with which the readings can be made on the compensator.

The compensation on the large field polariscope is achieved by the quarter wave plate method; the analyzer is rotated to obtain compensation, with a quarter wave plate between the analyzer and the plastic. A rotation of 180° causes one wave length retardation which corresponds to one fringe. The scale can be read at every two degrees. Thus the smallest change which can be still observed is one ninetieth of a fringe.

The oblique incidence polariscope and the polarizing microscope have a quartz wedge compensator. For this a 35 division scale corresponds to one fringe change. It can be read at each half graduation and therefore the smallest change to be noticed will be one seventieth of a fringe.

Up to this point the reinforcing effect of the plastic was not included in the equations determining the stresses in the structure. An investigation by Zandman, Redner and Riegner (21) showed that for thin coating in plane stress this reinforcing effect is negligible. In case of bending or combined stresses or when the thickness of the coat is not small compared to the thickness of metal this reinforcing effect can not be neglected and must be accounted for. The influence of the coat on the strains and so on birefringence

is given as a correction factor plotted as a function of the ratio of plastic thickness to metal thickness in the above mentioned reference. This correction factor is especially important when thin plates are subjected to bending.

Description of the Pressure Vessel and Equipment Used.

The structure under investigation was a small pressure vessel obtained commercially (Fig.4). Two torispherical dished heads were welded to a cylinder, which was rolled from a steel plate and welded along the generating line. One head was complete; the other contained two tapped holes for filling and pressurizing the vessel.

The photoelastic investigation was made on the complete head, and to avoid reinforcing at the joint of this head to the cylinder, the weld was ground flush to the parent materials outside and inside. Care was taken also that the cylinder was sufficiently long so that the other end closure had no effect on the stresses in the head under investigation.

The material of the vessel was mild steel with a yield strength of 30000 psi. The modulus of elasticity was 30×10^6 psi.

The wall thickness, one eighth of an inch, was uniform in the heads and the cylinder, and since the radius of the torus (knuckle) part of the head was small, this part of the vessel could not be considered as a thin shell. The ratio of the radius of curvature to the wall thickness was 3.84 and the ratio for thin shells is defined as above is ten. The

other parts, the spherical cap and the cylinder, were thin shells having a radius of curvature to thickness ratio of 64 and 32 respectively.

To make the photoelastic measurements easier, the vessel was mounted on a stand and provisions was made so that it could be rotated about an axis at the mid length of the cylinder (Fig.6,7).

Due to the double curvature of the head of the pressure vessel it was necessary to use the moulding technique (17) to cover it with a plastic layer, as described in Appendix II.

A partially polymerized plastic sheet was obtained by casting liquid plastic on a level glass surface. This sheet showed no resistance against forming and was formed on the head without introducing initial birefringence. When the plastic hardened, it was cemented to the head by an epoxy resin cement (19).

The strain optical coefficient of the plastic was obtained by calibration using a calibration strip from the cast plastic. A detailed description of the calibration is given in the Appendix.

The pressure vessel was filled with water which had been in the open air before filling to release the absorbed air. A high pressure rubber hose provided the connection between the pressure vessel and a dead weight tester (Fig.6), which produced the required pressure. Before applying any pressure,

the system was bled of air at the highest point.

The dead weight tester remained connected to the pressure vessel throughout the tests and its piston was rotated to secure uniform pressure while the photoelastic measurements were taken. All measurements were taken at 500 psig.

The photoelastic part of the experiment consisted of the investigation of a set of points along a radial line from the center of the head to the cylinder, defined by the angle α (Fig.4). Measurements were taken at every degree from $\alpha = 0^{\circ}$ to $\alpha = 20^{\circ}$ and at every four degrees from $\alpha = 20^{\circ}$ to $\alpha = 90^{\circ}$

Instruments used were the large field polariscope,which was used to determine the directions and the difference of the principal stresses (Fig.7), the oblique incidence polariscope, which supplied the values for the individual principal stresses (Fig.8), and the polarizing microscope, which provided control values to check the values obtained by the large field polariscope (Fig.9).

When calculating the stresses a correction factor for bending had to be introduced, because bending moment existed in the torus due to the internal pressure. The correction factor was obtained from Fig 2 in reference (21) for the existing ratio of plastic to metal thickness.

Results.

The directions of the principal stresses were established first with the use of the large field polariscope without the quarter wave plates. It was found that within a circle drawn at $\alpha = 32^{\circ}$ around the axis of the shell on the spherical cap, every point was isotropic, i.e. the principal stresses were equal in all directions.

Another dark ring appeared in the field of the polariscope at $\alpha = 10^{\circ}$ where the points proved to be singular, which meant that both principal stresses became zero.

At the other parts of the head a radial dark line coinciding always with the polarizing axis of the polarizer plate indicated that the direction of the principal stresses were meridional and circumferential respectively (Fig.10). The mathematically larger principal stress, σ_1 was circumferential between $\alpha = 0^{\circ}$ and $\alpha = 10^{\circ}$; and changed to meridional between $\alpha = 10^{\circ}$ and $\alpha = 32^{\circ}$

These observations led to the conclusion that the meridional and circumferential stresses along a radial line were the principal stresses, and so the maximum of meridional and circumferential stresses were determined, giving the maximum stresses at the point.

As part of the quantitative analysis normal and oblique

incidence measurements were taken.

When the plastic was viewed with the large field polariscope set for circularly polarized light field, three areas showed dark patterns. One area was within the circle drawn at $\alpha = 32^{\circ}$ around the axis of the shell on the spherical cap. The other was a ring at $\alpha = 10^{\circ}$, and the third another ring at $\alpha = 0^{\circ}$. Due to the circularly polarized light field, these dark areas indicated that the difference of the principal stresses was zero there. Further investigation however showed that the points on the ring at $\alpha = 10^{\circ}$ were singular, and the points on the spherical cap within the circle at the angle $\alpha = 32^{\circ}$ and the points on the ring at $\alpha = 0^{\circ}$ were isotropic.

The fringe value increased from $\alpha = 0^{\circ}$, reached its maximum at $\alpha = 5.5^{\circ}$, then decreased to zero at $\alpha = 10^{\circ}$. It increased again from $\alpha = 10^{\circ}$ to $\alpha = 17^{\circ}$ and decreased to zero at $\alpha = 32^{\circ}$. The difference of the principal strains did not reach one fringe at any point from $\alpha = 0^{\circ}$ to $\alpha = 90^{\circ}$ which means that the retardation measured was always less than one wave length of, the white light.

Oblique incidence measurements were made after the direction of the principal stresses was determined with the large field polariscope. The plane of incident and reflected light of the oblique incidence polariscope was first aligned to coincide with a meridional line and the readings so ob-

tained were used to determine the individual circumferential stress. Similarly it was aligned perpendicular to the previous direction to supply the values for the calculation of the meridional stresses. Each measurement was taken when the pressure vessel was loaded and again when it was unloaded. The sign of the compensator values was defined by their location from the zero fringe in the compensator wedge and by the algebraic subtraction of the no load reading from the reading taken under load.

A dimensionless stress intensity factor was defined as the ratio of the stress measured to the circumferential stress in the cylinder remote from the end closures

$$\text{Stress Intensity} = \frac{\sigma}{\frac{pR_c}{t_c}}$$

where σ = stress measured

p = pressure in the vessel

R_c = radius of the cylinder

t_c = wall thickness of the cylinder

This stress intensity factor is given with the stress values at each point on the head in Table I. The points on the head were defined by the angle α, but the corresponding values for the angle ϕ were also included, because it was found that this angle was more often used in the literature.

The stresses were also plotted on lines perpendicular to the head at each point (Fig.11), and in a coordinate system of angle α versus the stresses (Fig.12).

The maximum meridional stress of σ_ϕ = -48500 psi occurred in the torus part of the head at α = 5.5°, while the maximum circumferential stress reached its maximum value of σ_θ = -33500 psi at α = 5°. Both stresses were compressive on the outer surface of the head.

Table I.

Meridional and Circumferential Stresses in the Head of the Pressure Vessel and the Corresponding Stress Intensity Factors.

Points defined by angles		Stresses 10^4 psi		Stress Intensity Factors	
α	ϕ	Circum-ferential	Meridional	Circum-ferential	Meridional
0.0	90	-2.00	-2.00	-1.25	-1.25
1.0		-2.65	-2.90	-1.66	-1.81
1.2	80	-2.70	-3.05	-1.69	-1.91
2.0		-2.95	-3.50	-1.84	-2.19
2.4	70	-3.00	-3.75	-1.88	-2.34
3.0		-3.20	-4.05	-2.00	-2.53
3.5	60	-3.25	-4.30	-2.03	-2.69
4.0		-3.30	-4.50	-2.06	-2.81
4.5	50	-3.30	-4.70	-2.06	-2.94
5.0		-3.35	-4.78	-2.10	-2.98
5.5	40	-3.30	-4.85	-2.06	-3.03
6.0		-3.18	-4.75	-1.99	-2.97
6.3	30	-3.10	-4.70	-1.94	-2.94
7.0	28	-2.85	-4.45	-1.78	-2.78
8.0		-2.50	-3.65	-1.56	-2.28
8.4	27	-2.35	-3.30	-1.47	-2.06
9.0		-2.10	-2.65	-1.31	-1.66
10.0	26	-1.50	-1.50	-0.94	-0.94

Table I. (continued)

Points defined by angles		Stresses 10^4 psi		Stress Intensity Factors	
α	ϕ	Circum-ferential	Meridional	Circum-ferential	Meridional
11.0	25	-0.85	0.00	-0.53	0.00
12.0		-0.20	1.00	-0.13	0.63
12.6	24	0.10	1.50	0.06	0.94
13.0		0.55	1.80	0.34	1.12
14.0	23	0.70	2.60	0.44	1.63
15.0		0.95	2.75	0.59	1.72
15.4	22	1.05	2.85	0.66	1.78
16.0		1.20	2.95	0.75	1.84
17.0	21	1.30	3.10	0.81	1.94
18.0		1.40	3.15	0.88	1.97
18.6	20	1.41	3.10	0.88	1.94
19.0		1.42	3.07	0.84	1.92
20.0	19	1.45	2.95	0.90	1.84
22.4	18	1.50	2.60	0.94	1.63
24.0	17	1.47	2.35	0.92	1.47
27.0	16	1.35	1.80	0.84	1.12
28.0		1.30	1.65	0.81	1.03
30.0	15	1.15	1.40	0.72	0.88
32.0	14	0.97	1.18	0.61	0.74
36.0		0.86	0.94	0.54	0.59
⋮	⋮	⋮	⋮	⋮	⋮
54.0	7	0.71	0.76	0.44	0.48
⋮	⋮	⋮	⋮	⋮	⋮
90.0	0	0.57	0.59	0.36	0.37

Comparison with other works on pressure vessel heads.

In order to assess the accuracy of the present stress investigation, the results were compared to values obtained in the literature. These values were arrived at by calculations, using the thin shell theory, and the dimensions of the vessel satisfied the conditions of thin shells.The vessel in the present investigation was not a thin shell. Therefore the distribution of the stresses and the maximum stress intensity factors were compared.

The heads in two of the work used as comparisons were torispherical and one was ellipsoidal.

The ellipsoidal head investigation was published by Kraus, Bilodeau and Langer (24). Results were presented in this paper for an ellipsoidal head having a two to one ratio of the major and minor axes.

Stress intensity indexes were tabulated for a series of vessels determined by parameters β, $\frac{D}{t}$, and $\frac{T}{t}$.

Where β = ratio of the major axis to the minor axis of the ellipsoidal head

D = diameter of cylinder

t = cylinder thickness

T = head thickness

For comparison β in the present investigation was taken as the ratio of the radius of the cylinder to the height of the head. The maximum stress intensity factor in reference (24) was 3.00 in the knuckle and 2.15 in the spherical cap. The parameters were $\beta = 3$ $\frac{D}{t} = 50$ $\frac{T}{t} = 1$ In the present investigation these parameters were $\beta = 3$ $\frac{D}{t} = 64$ $\frac{T}{t} = 1$ and the maximum stress intensity in the knuckle was 3.00 and in the spherical cap 2.28.

The papers dealing with the torispherical heads were published by Galletly (22,23).

One of these papers (23), shows that the ASME Code for Unfired Pressure Vessels gives very low stress values in the torus. The calculations were based on the solution of the differential equations for constant thickness shells of revolution, The results show the distribution of the meridional bending stresses and the circumferential direct stresses in the torus, and that both stresses exceeded the yield point of the material.

The comparison of these results to the results obtained in the present investigation (Fig.13) are made on the base of the stress intensity factor. Good agreement prevails for the maximum stress intensity factor, and for the sign of the stresses.

The dimensions of the head were

Radius of spherical cap	227.5	in
Radius of the cylinder	138.23	in
Thickness of the head	0.625	in
Thickness of the cylinder	0.460	in
Pressure	60	psig.

The second paper (22) gives two examples in which pressure vessels of different shapes were designed with the use of influence coefficients. It showed also that high stresses occurred in the tori. The stress distribution in the torus was presented and this was also compared to the values presently obtained in (Fig.13).

The dimensions of the head were:

Radius of the spherical cap	281.25	in
Radius of the cylinder	150	in
Thickness of the head	0.625	in
Thickness of the cylinder	0.5	in
Pressure	60	psig.

The stress due to internal pressure in a torispherical head was also determined in the presently investigated vessel by using the ASME Code for Unfired Pressure Vessels.

The equation used was

$$\sigma = \frac{p}{\eta} \left(0.5\ M \frac{R}{t} + 0.1 \right)$$

where σ = stress in the wall

p = internal pressure

R = inside radius of the spherical cap

t = thickness of the head

η = joint efficiency (unity)

M = 1.77, when the radius of the knuckle is 6 % of the radius of spherical cap.

The stress was

$$\sigma = 28400 \text{ psi}$$

and the stress intensity factor was 1.78.

The distribution curve was flatter for the present investigation which was attributed to the wall thickness of the torus.

Summary and Conclusions.

The photoelastic coating method provided a new approach for evaluating the stresses in the torispherical head of a pressure vessel. The coat applied to the surface made possible the determination of the strains on the surface of the structure. It also supplied the directions of the principal stresses. In this case they were circumferential and meridional.

The maximum value and the location of the stresses as well as their sign was determined and these values agreed closely with the values obtained in other investigations. The circumferential stress distribution was lower in the present investigation than the distribution in the compared works. This was attributed to the thicker torus in the pressure vessel investigated.

The maximum value of the stresses exceeded the yield point of the material, although no yielding was noticed during the test. It is believed that previous unsuccessful testing caused work hardening in the material.

The thickness of the plastic determined the sensitivity of the measurements and in the present case it was quite low. A thicker coating increases the sensitivity, but the reinforcing effect also increases. The casting and forming of the thicker sheet is also more difficult.

When liquid plastic is cast, quite large quantities should be mixed with the accelerator to obtain a uniform polymerization. The amount of accelerator added is very vital; a little deviation from the required proportion causes non uniform sheet formation.

This, and the forming of thick coatings on curved surfaces could be investigated in a separate work. Photoelastic measurements on a shell of revolution in which the stresses were obtained analytically would be also valuable.

In conclusion the casting method proved to be a very useful method for evaluating the stresses in the pressure vessel. The instruments used can be easily carried and thus photoelastic investigation is possible even on the site, provided an electric outlet is available. The coating of the structure requires little equipment and a short time only.

References.

1., Mesnager, M., "Sur la determination optique des tensions intervenuer dans les solides a trois dimensions" Comptes Rendus l'Acad. Sci., 190, 1249, Paris, (1930)

2., Mabboux, G., "Applications de la Photoelasticite dans les ouvrages en beton," Editors: Delmar, Chapon Grounouihou, France (1933)

3., Oppel, G., "Das Polarizationsoptische Schichtverfahren zur Messung der Oberflachenspannung am beanspruchten Bauteil ohne Modell," VDI-Zitschrift Bd. 81 Nr. 27, (1937)

4., D'Agostino, J., Drucker, D.C, Liu, C.K. and Mylonas, C., "An analysis of plastic behaviour of metals with bonded birefringent plastic," Proceedings of The Society for Experimental Stress Analysis. Vol. XII. 2, 115-122.(1955)

5., D'Agostino, J., Drucker, D.C, Liu, C.K. and Mylonas, C., "Epoxy adhesives and casting resins as Photoelastic plastics" Proceedings of The Society for Experimental Stress Analysis. Vol. XII. 2, 123-128. (1955)

6., Zandman. F., "Analyse des contraintes par vernis photoelastiques," Groupment l'Advancement Methodes d'Anal-Contraintes Vol. 2, No. 6 1-12 (1956)

7., Zandman, F., "Mesures photoelastiques des deformations elastiques et plastiques et des fragmentations cristallines dans les metaux," Revue de Metallurgie Vol. LII. No. 8. 638-642 (1956)

8., Zandman, F.,and Wood, M.R., "Photo-Stress a new technique for photoelastic stress analysis for observing and measuring surface strains on actual structures and parts" Product Engineering. 167-178 (1956)

9., Zandman, F., "Photoelastic-Coating technique for determining stress distribution in welded structures," Welding Journal Research Supplement (May 1960)

10., Frocht.,M.M., Photoelasticity. New York. John Wiley & Sons Inc. (1948) Vol. I. and II.

11., Hetenyi, H.,(ed) Handbook of Experimental Stress Analysis New York. John Wiley & Sons Inc. (1950)

12., "INSTRUCTIONS for the use of Photostress Large Field Universal Meter" Tatnall Measuring Systems Co.Bulletin. (Phoenixville) No. 8005.(1958)

13., Mindlin, R.D., "Distortion of the photoelastic fringe-pattern in an optically unbalanced polariscope." ASME Trans. Vol. 59. No. A 170 (1937)

14., Timoshenko, S., Goodier, J.N., Theory of Elasticity Engineering Societies Monograph., McGraw-Hill Book Co. Inc. New York. Second ed. (1951)

15., McMaster, R.,(ed) Nondestructive Testing Handbook. New York. The Ronald Press Co., (1959) Vol II.

16., "Operating instructions for the Oblique Incidence Meter" Tatnall Measuring System Co. Bulletin (Phoenixville) No. BN-8003 (1958)

17., "Suggestions for plastic selection." Tatnall Measuring System Co. Bulletin (Phoenixville) No. BN-8022 (1959)

18., "Instructions for Applying Photostress Liquid Plastic" Tatnall Measuring System Co. Bulletin. (Phoenixville) No. 8005 (1958)

19., "Instructions for moulding contoured sheets of photo-stress plastic" Tatnall Measuring System Co.Bulletin. No. IB-8008

20., "Instructions for applying photostress sheet plastic" Tatnall Measuring System Co. Bulletin. (Phoenixville) No. IB-8004 (1959)

21., Zandman, F., Redner, S.S., and Riegner, E.I., "Reinforcing effect of birefringent coatings"Proceedings of The Society for Experimental Stress Analysis No.588.(1959)

22., Galletly, G.D., "Influence coefficirnts and pressure vessel analysis," Journal of Engineering for Industry ASME Trans, Ser. B. Vol 82 259-269 (1960)

23., Galletly, G.D., "Torispherical shells-A caution to designers." Journal of Engineering for Industry. ASME Trans. Ser. B. Vol. 81. 51-66 (1959)

24., Kraus, H., Bilodeau, G.G., Langer, B.F., "Stresses in thin-walled pressure vessels with ellipsoidal heads." Journal of Engineering for Industry. ASME Trans. Ser. B. Vol. 83. 29-42 (1961)

Appendix I.

The Mathematical Theory.

Normal Incidence.

The connection between the principal stresses in a bi-refringent material and the retardation obtained between the ordinary and extraordinary rays of a polarized light is expressed in Neumann's law for plane stresses.

$$\delta_n = C\,(\sigma_1 - \sigma_2)_p\,2\,t \qquad 1.$$

Where σ_1; σ_2 are the principal stresses in the plastic
δ_n relative retardation
C stress optical coefficient
t thickness

Rewriting to give the difference of the principal stresses

$$(\sigma_1 - \sigma_2)_p = \frac{\delta_n}{C\,2\,t} \qquad 2.$$

The difference of the principal stresses can also be expressed as

$$(\sigma_1 - \sigma_2)_p = \frac{E_p}{1 + \nu_p}\,(\epsilon_1 - \epsilon_2)_p \qquad 3.$$

Where E = Modulus of Elasticity

ν = Poisson's ratio

ϵ_1; ϵ_2 = Principal Strains

Combining equations 2 and 3

$$\frac{\delta_n}{C\ 2\ t} = \frac{E_p}{1 + \nu_p} (\epsilon_1 - \epsilon_2)_p \qquad 4.$$

or

$$(\epsilon_1 - \epsilon_2)_p = \frac{\delta_n}{C\ E_p} \frac{(1 + \nu_p)}{2\ t} \qquad 4/a$$

Denoting

$$\frac{CE_p}{1 + \nu_p} = K$$

equation 4/a becomes

$$(\epsilon_1 - \epsilon_2)_p = \frac{\delta_n}{2\ t\ K} \qquad 5.$$

Where K = is the strain optical coefficient and is usually determined by calibration

Assuming a good bond between the plastic coat and structure

$$(\epsilon_1 - \epsilon_2)_p = (\epsilon_1 - \epsilon_2)_w \qquad 5/a$$

and the difference of the principal strains in the structure

is given by

$$(\epsilon_1 - \epsilon_2)_w = \frac{\delta_n}{2\ t\ K} \qquad 6.$$

To find the difference of the principal stresses Hooke's law is used

$$(\sigma_1 - \sigma_2)_p = \frac{E_w}{1 + \nu_w} \frac{\delta_n}{2\ t\ K} \qquad 7.$$

Therefore the determination of the relative retardation provided the difference of the principal stresses in the structure. From this the maximum shear stress is obtained

$$\tau_{max} = \frac{\sigma_1 - \sigma_2}{2}$$

The individual principal stress can be obtained also with one normal reading however, when the point under investigation is located at a discontinuity or free surface. At these points the normal stress must be zero and equation 7 gives the tangential stress.

Two equations are necessary to define the two individual stresses at points not on a free surface. These two equations can be obtained by taking two oblique readings or one normal and one oblique reading.

The Oblique Incidence.

As seen from the previous discussion, when the incidence of the light is normal, only the difference of the principal stresses can be obtained. Taking another reading under oblique incidence, the retardation observed will be the difference of the secondary principal stresses, thus giving another equation for solving the two principal stresses individually.

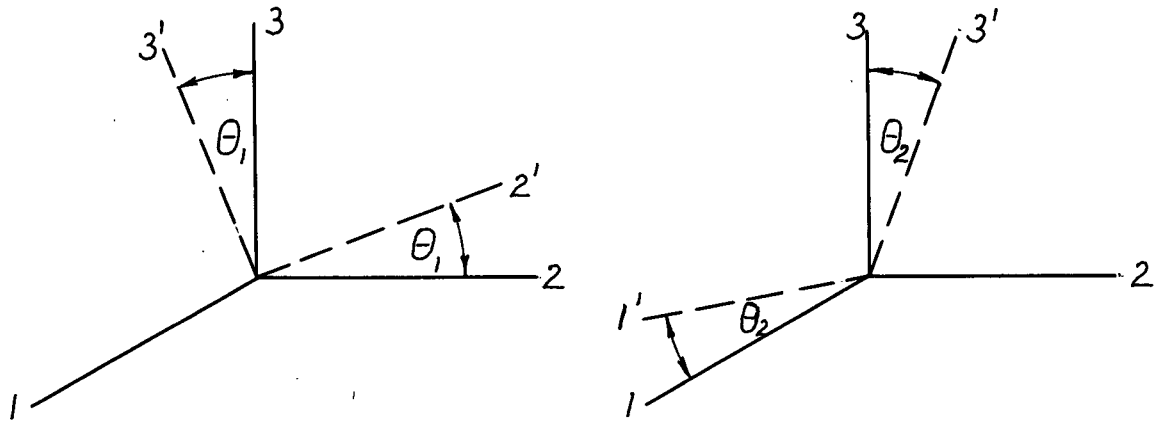

As the coordinate systems show, it can be always arranged that one of the principal stresses coincides with one axis of the secondary principal stresses. Since the directions of the principal stresses can be obtained with a normal incidence polariscope, the oblique incidence instrument can be aligned with one of these directions, thus including one principal stress in the difference of the secondary principal

stresses. Starting with Neumann's equation again and using Mohr's circle drawn for a three dimension case we can write the equations for the ratardation taking two oblique incidence measurements

$$(\sigma_1 - \sigma_2')_p = \frac{\delta_{o1}}{2\ t\ /\ \cos\theta_1\ C} \qquad 10.$$

$$(\sigma_2 - \sigma_1')_p = \frac{\delta_{o2}}{2\ t\ /\ \cos\theta_2\ C} \qquad 11.$$

where δ_{o1} and δ_{o2} are the retardations measured in oblique incidence the instrument being aligned with the direction of the proper principal stress. σ_1' σ_2' can be defined from Mohr's circle as shown

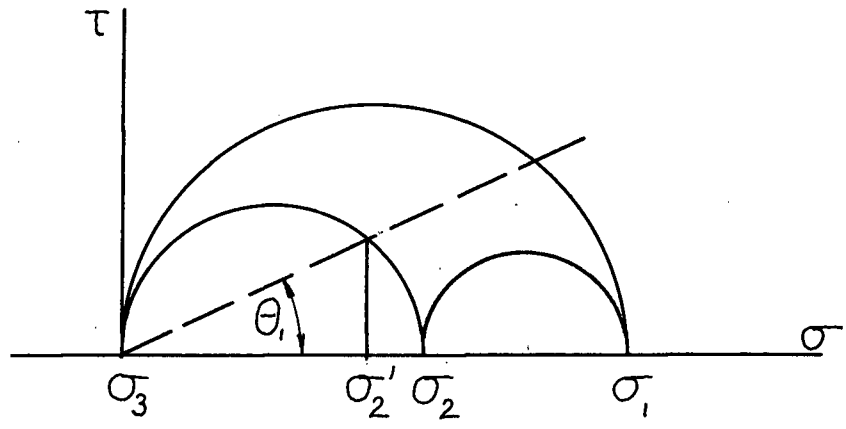

$$(\sigma_2')_p = (\sigma_2 \cos^2\theta_1)_p \qquad (\sigma_1')_p = (\sigma_1 \cos^2\theta_2)_p$$

therefore equation 10, and 11 can be expressed in terms of the principal stresses as follows

$$(\sigma_1 - \sigma_2 \cos^2 \theta_1)_p = \frac{\delta_{o1}}{2\ t\ /\ \cos \theta_1\ C} \qquad 12.$$

$$(\sigma_2 - \sigma_1 \cos^2 \theta_2)_p = \frac{\delta_{o2}}{2\ t\ /\ \cos \theta_2\ C} \qquad 13.$$

Solving these simultaneous equations for σ_1 and σ_2

$$(\sigma_1)_p = \frac{\dfrac{\delta_{o1}}{2\ t\ /\ \cos \theta_2\ C} + \dfrac{\delta_{o2} \cos^2 \theta_1}{2\ t\ /\ \cos \theta_1\ C}}{1 - \cos^2 \theta_2 \cos^2 \theta_1} \qquad 14.$$

$$(\sigma_2)_p = \frac{\dfrac{\delta_{o2}}{2\ t\ /\ \cos \theta_2\ C} + \dfrac{\delta_{o1} \cos^2 \theta_2}{2\ t\ /\ \cos \theta_1\ C}}{1 - \cos^2 \theta_2 \cos^2 \theta_1} \qquad 15.$$

Great simplification can be introduced by choosing the angle of incidence for both cases at $\theta_1 = \theta_2 = 45^\circ$ with which equations 14 and 15 become reduced to

$$(\sigma_1)_p = \frac{\sqrt{2}}{3\ t\ C} \left(\delta_{o1} + \frac{\delta_{o2}}{2} \right) \qquad 16.$$

$$(\sigma_2)_p = \frac{\sqrt{2}}{3\ t\ C}\left(\delta_{o2} + \frac{\delta_{o1}}{2}\right) \qquad 17.$$

Knowing from the normal incidence derivation that

$$K = \frac{C\ \ E_p}{1 + \nu_p}$$

and from this

$$C = \frac{K\ (1 + \nu_p)}{E_p}$$

Substituting this value of C into equations 16 and 17 and assuming that $(\epsilon_1)_p = (\epsilon_1)_w$ and $\nu_p = \nu_w$ From Hooke's law

$$(\sigma_1)_w = \frac{\sqrt{2}\ E_w}{3\ t\ K\ (1 + \nu_p)}\left(\delta_{o1} + \frac{\delta_{o2}}{2}\right) \qquad 18.$$

$$(\sigma_2)_w = \frac{\sqrt{2}\ E_w}{3\ t\ K\ (1 + \nu_p)}\left(\delta_{o2} + \frac{\delta_{o1}}{2}\right) \qquad 19.$$

As stated earlier it is not necessary that the oblique incidence reading be taken to determine the individual principal stresses. One oblique reading with the normal reading would be sufficient. If an oblique reading is taken for a retardation value including the principal stress σ_1, the equation become

$$(\sigma_1 - \sigma_2)_p = \frac{\delta_n}{2\ t\ C} \qquad 20.$$

$$(\sigma_1 - \sigma_2')_p = (\sigma_1 - \sigma_2 \cos^2 \theta_1)_p = \frac{\delta_{o1}}{2\ t\ /\ \cos \theta_1\ C} \qquad 21.$$

Solving these equations for σ_1 and σ_2 the equations determining the stresses in the structure will be

$$(\sigma_1)_w = \frac{E_w}{t\ K\ (1 + \nu_p)} \left(\frac{\sqrt{2}}{2}\ \delta_{o1} - \frac{\delta_n}{2}\right) \qquad 22.$$

$$(\sigma_2)_w = \frac{E_w}{t\ K\ (1 + \nu_p)} \left(\frac{\sqrt{2}}{2}\ \delta_{o1} - \delta_n\right) \qquad 23.$$

Similarly the equations determining the stresses in the structure when the oblique reading includes the principal stress σ_2 are

$$(\sigma_1)_w = \frac{E_w}{t\ K\ (1 + \nu_p)} \left(\frac{\sqrt{2}}{2}\ \delta_{o2} - \delta_n\right) \qquad 24.$$

$$(\sigma_2)_w = \frac{E_w}{t\ K\ (1 + \nu_p)} \left(\frac{\sqrt{2}}{2}\ \delta_{o2} - \frac{\delta_n}{2}\right) \qquad 25.$$

The retardation in the case of normal incidence of light was determined from the equation

$$\delta_n = (k + \frac{\beta}{180})\lambda$$

where k is any positive number (0,1,2,...)

β is the compensator reading

λ is the wave length of light used

and in the case of oblique incidence

$$\delta_{o1} = \frac{m_1 \lambda}{35}$$

where m_1 is the difference of the compensator readings under load and no load

Equations 18 and 19 are expressed in a simpler form by introducing the numerical values for the wave length of the white light and Poisson's ratio as

$\lambda = 2.27 \times 10^{-5}$ in

$\nu = 0.3$

$$(\sigma_1)_w = 2.36 \times 10^{-7} \frac{E_w}{tK} (m_1 + \frac{m_2}{2})$$

$$(\sigma_2)_w = 2.36 \times 10^{-7} \frac{E_w}{tK} (m_2 + \frac{m_1}{2})$$

Appendix II.

Casting plastic sheets for the head of the vessel.

To cover the head with the photoelastic plastic, a contoured sheet had to be used. The sheet was formed on the head by using a partially polymerized plastic sheet. This partially polymerized sheet was obtained by casting plastic on an accurately levelled glass plate, the surface of which was protected by a layer of silicone varnish. This layer was to prevent the plastic from sticking to the glass,and was baked on the glass in an oven at 450°F for four hours. A hardboard frame, one quarter of an inch thick, and 9" x 9" inside dimensions was put on the glass and sealed with masking tape around its external perimeter. Seventy grams of liquid photoelastic plastic was mixed with fifteen per cent by weight hardener and allowed to reach an exotherm temperature of 110° F. It was then poured onto the prepared glass surface, where the polymerization began. After three and a half hours at room temperature the plastic formed a sheet of uniform thickness, which was very soft. The sheet was then formed on the head, covering more than one third of it. No birefringence was introduced while forming. The edges of the sheet were held in position with lightly applied scotch tape, and left for completion of the polymerization which required

about 24 hours.

When the polymerization of the plastic was completed, the contoured sheet was removed from the head and its thickness measured to one ten thousandth of an inch, with a micrometer. The edges were cut and the surface cleaned with acetone.

A reflective type cement was used to bond the photoelastic sheet to the surface of the head. The cement was mixed with the hardener, ten per cent by weight, and allowed to set for ten minutes or more. A layer of about one sixteenth of an inch was then spread on the head from the mixed cement and the sheet was applied. Air bubbles were pressed out by applying the sheet at an angle to the surface and gradually lowering so that the excess cement squeezed out with the air at the other end. The edges of the plastic were sealed with the remaining cement. The bond hardened in about a day, and the coat was ready for the photoelastic test.The same procedure was used to bond the calibration strip to the calibration bar.

Appendix III.

Determination of the strain optical coefficient by calibration.

After the thickness of the plastic calibration strip had been measured the strip was bonded to an aluminum bar. The hardening of the bond took place at room temperature and completed in twenty four hours. Before the calibration was started, the plastic was examined with a polariscope and it was observed that no initial birefringence existed before loading the test bar. One end of the bar was then clamped to a bench and provision was made to load it at the other end (Fig.14). After the large field polariscope was positioned for the readings, the test bar was loaded in two pound increments and the retardations noted for each load. The points were plotted in a compensator readings versus load coordinate system (Fig.15). From the straight line relationship between load and retardation, the load causing a retardation equivalent to one wave length of the white light used was determined. The difference of the principal strains corresponding to this retardation is called the fringe value of the plastic. This fringe value is not equal to the actual strain difference when the structure is bent, because of the reinforcing effect of the plastic (20), and a correction factor must be applied.

The difference of the principal strains was also determined by calculation, using the well known equations from the theory of elasticity.

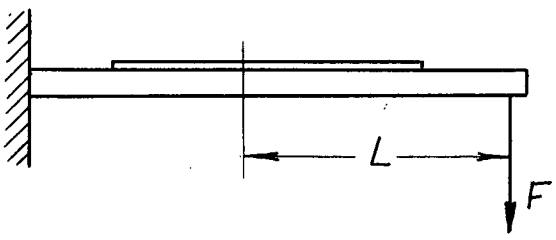

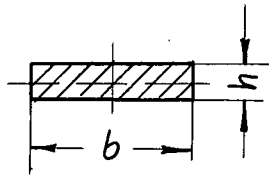

The tensile stress resulting from the load will be principal stress at the top surface of the bar, the other principal stress is zero.

$$\sigma_1 = \frac{M}{Z}$$

$$\sigma_2 = 0$$

The difference of the principal strains as derived earlier, is given by

$$\epsilon_1 - \epsilon_2 = \frac{1 + \nu}{E} (\sigma_1 - \sigma_2)$$

But from the above $\sigma_2 = 0$ and

$$\epsilon_1 - \epsilon_2 = \frac{\sigma_1}{E} (1 + \nu)$$

As stated earlier, a correction factor was necessary to take care of the birefringence caused by bending. Introducing this into the equation

$$\epsilon_1 - \epsilon_2 = \frac{\sigma_1}{E} (1 + \nu) C_2$$

This equation gives the fringe value from the strains occurring at the surface of the test bar. Since the strains are the same in the plastic as in the metal at the interface, this fringe value was made equal to the fringe value given by equation 9 in Appendix I.

$$\epsilon_1 - \epsilon_2 = \frac{\sigma_1}{E} (1 + \nu) C_2 = \frac{\delta}{2 t K}$$

expressing the strain optical coefficient from here

$$K = \frac{\delta}{2 t \frac{\sigma_1}{E} (1 + \nu) C_2}$$

In the present case the values were

δ =	2.27×10^{-5}	in
t =	0.052	in
F =	25.5	lb
L =	6.0	in
Z =	1.04×10^{-3}	in^3
E =	30.0×10^6	lb/in^2
ν =	0.3	
C_2 =	1.16	

$b = 1.0$ in

$h = 0.25$ in

and so $\underline{K = 0.0905}$

with this value of K the fringe value of the plastic was

$\underline{f = 2400 \times 10^{-6} \text{ in/in}}$

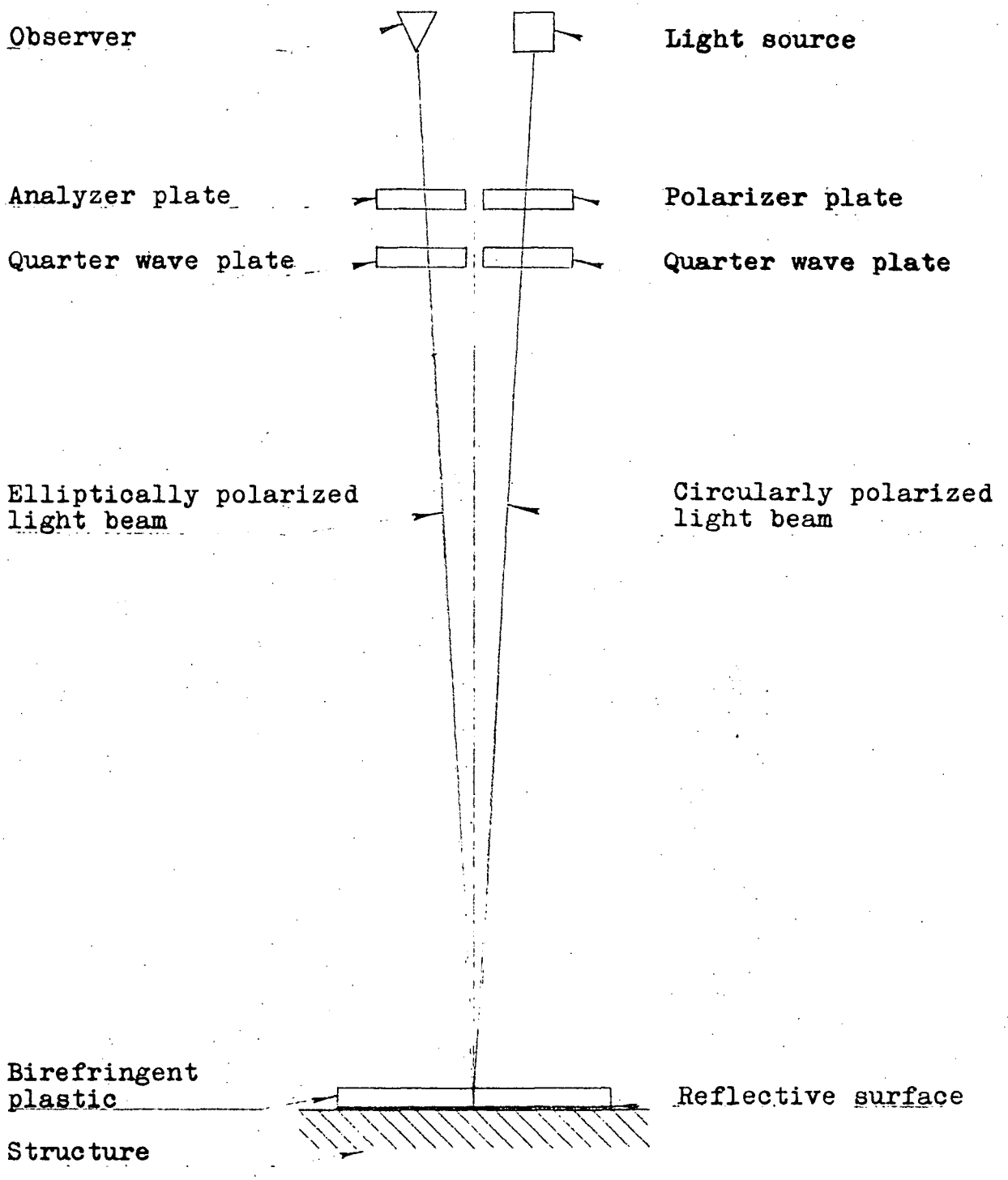

Fig. 1. Schematic drawing of Reflection polariscope

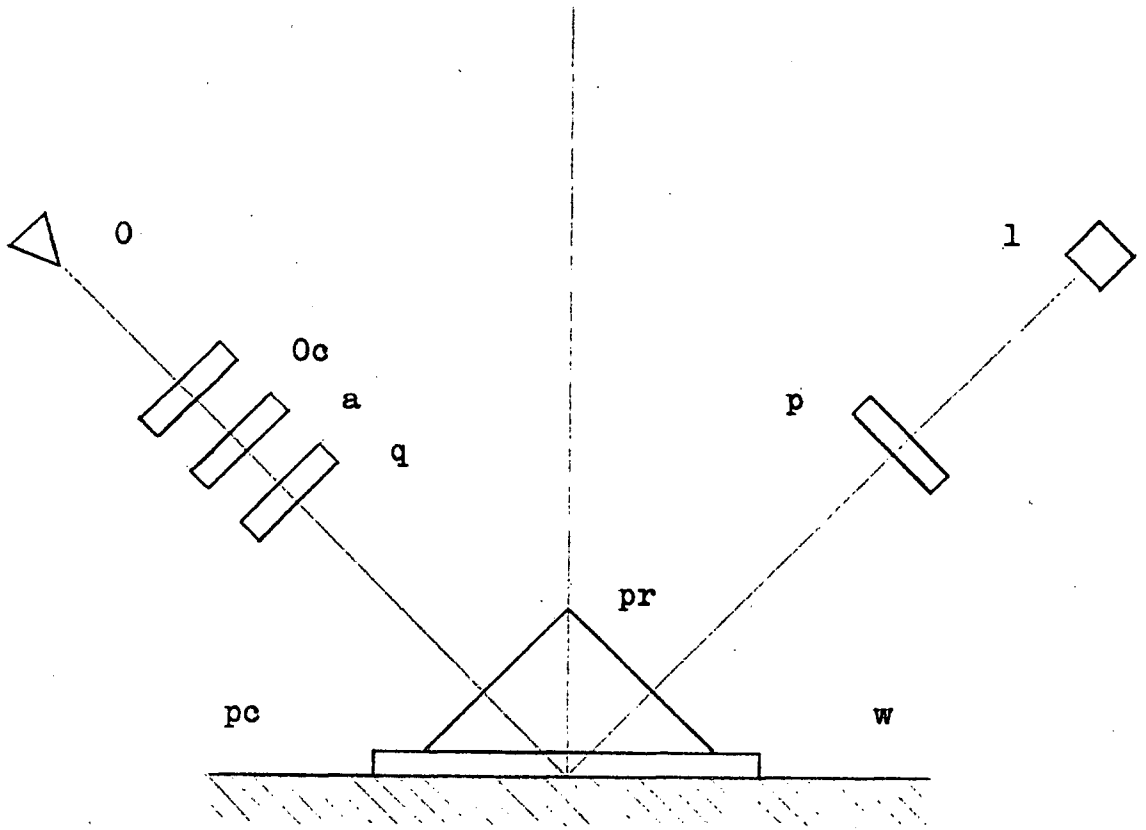

O = Observer
Oc = Ocular
a = Analyzer plate
q = Quartz wedge compensator

l = Light source
p = Polarizer plate
pr = Prism
w = Structure
pc = Plastic coat

Fig.2. Schematic of Oblique Incidence Polariscope

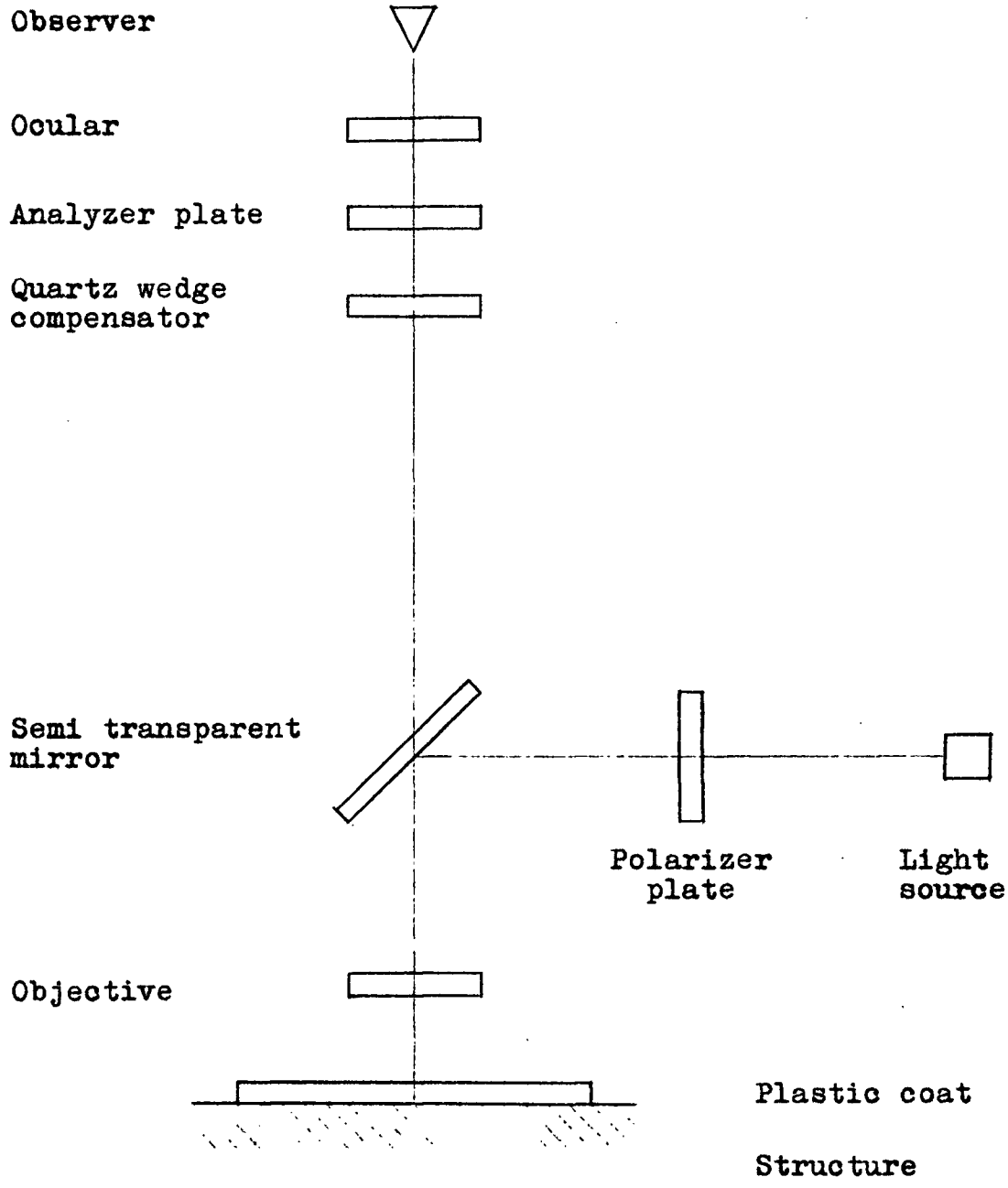

Fig.3. Schematic of Polarizing Microscope

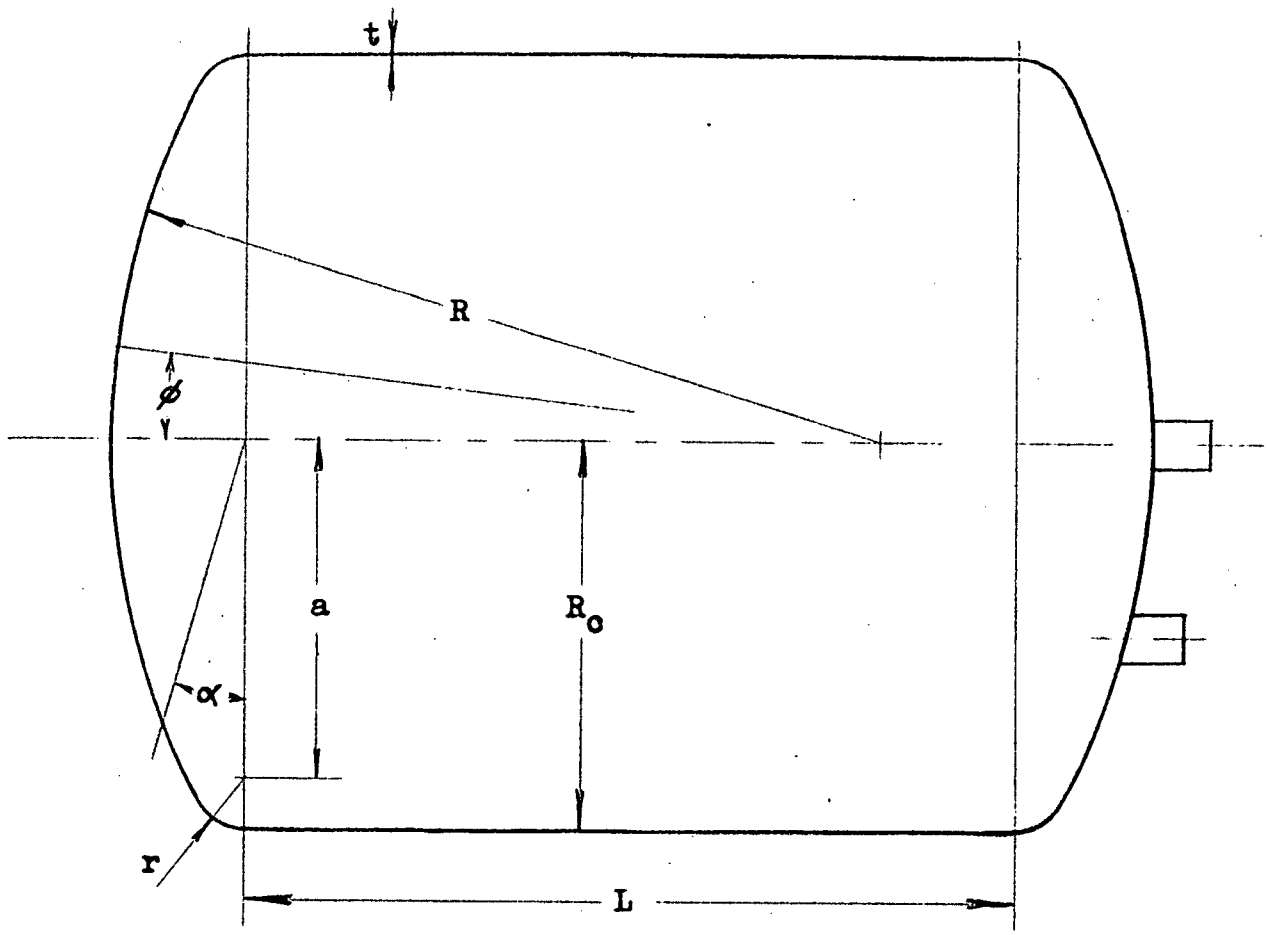

$R = 8.0$ in
$R_c = 4.0$ in
$L = 8.0$ in
$r = 0.48$ in
$t = 0.125$ in

Fig.4. The Pressure Vessel

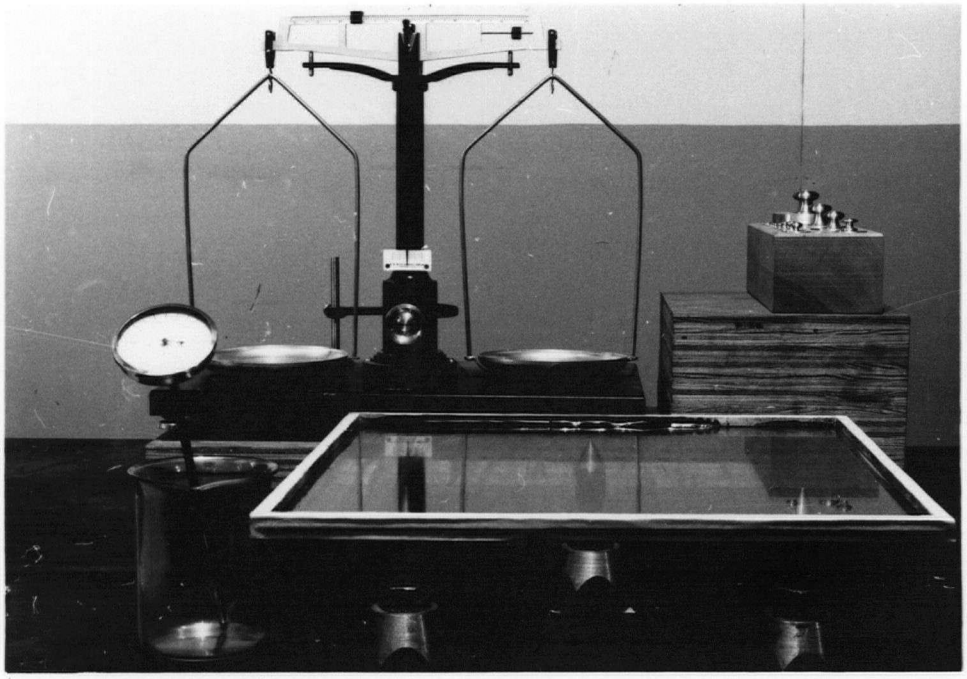

Fig.5. Casting of Plastic

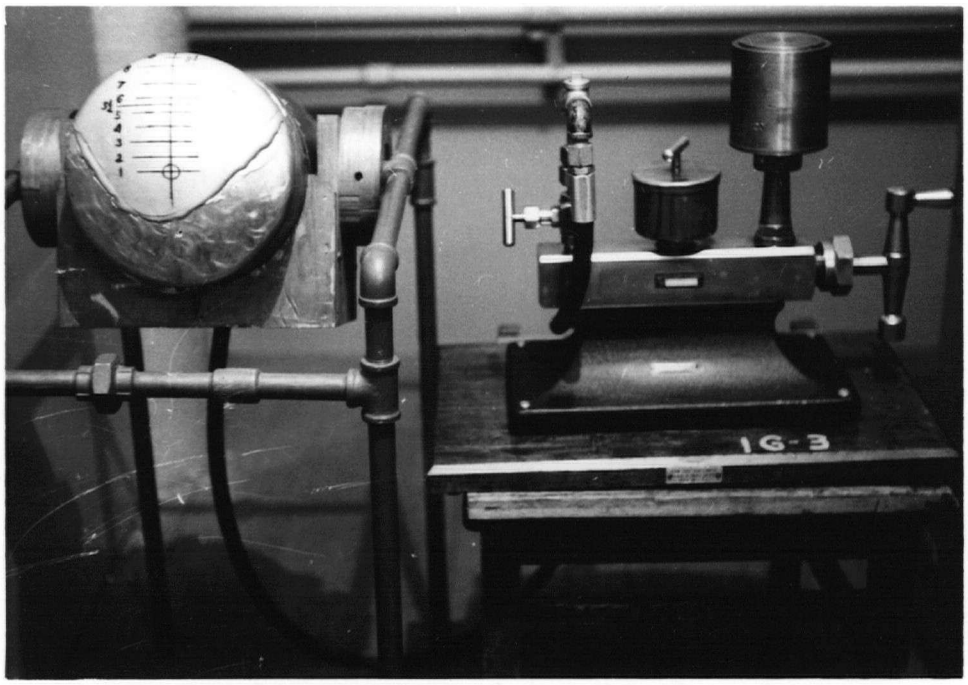

Fig.6. Pressure Vessel and Dead Weight Tester

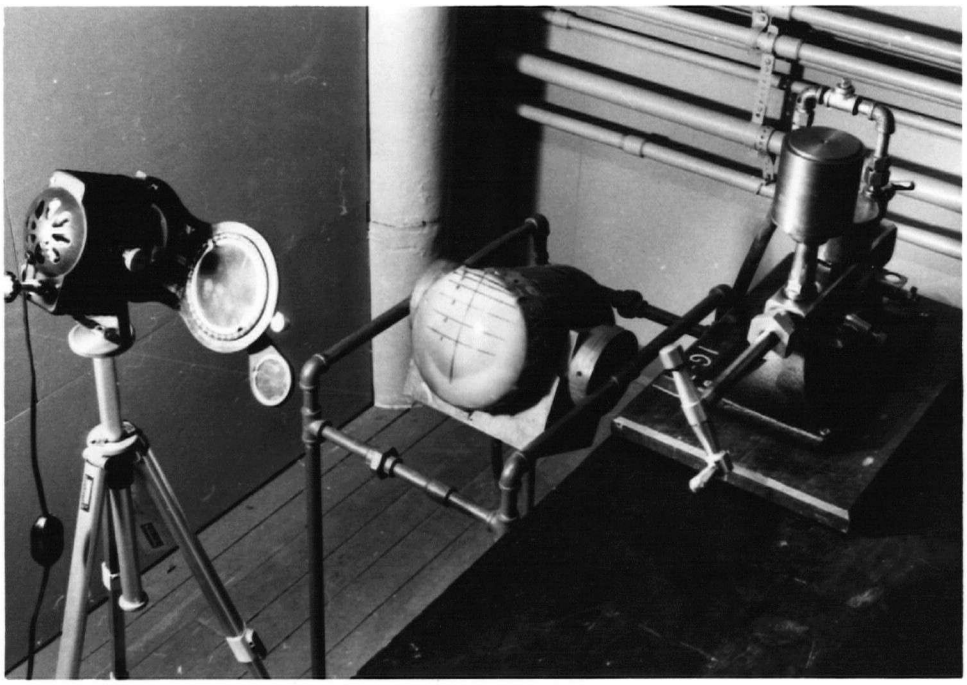

Fig.7. Test Setup for the Large Field Polariscope

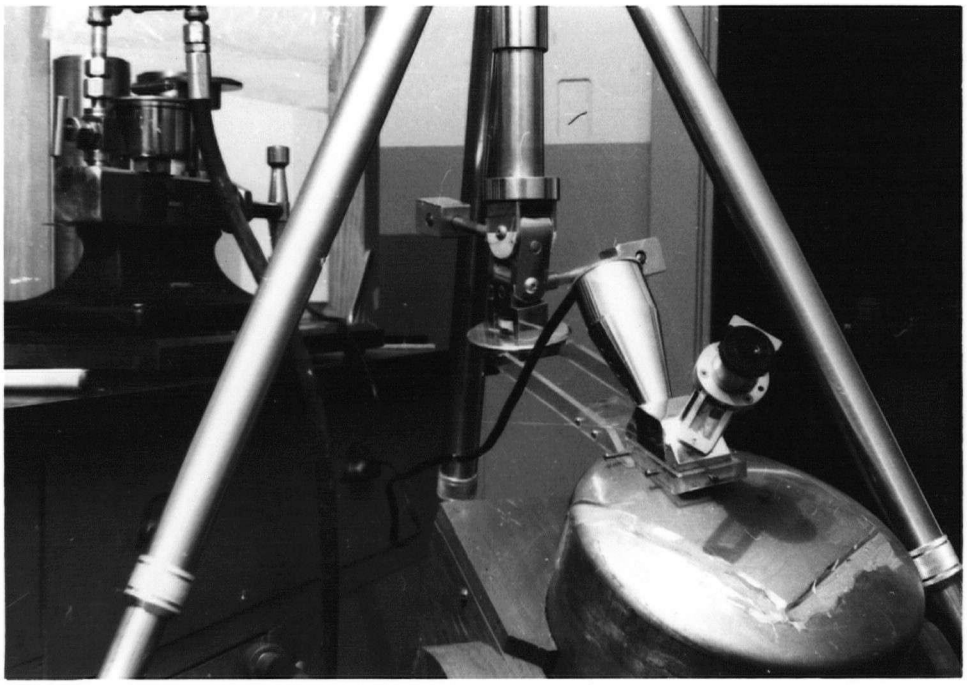

Fig.8. Test Setup for the Oblique Incidence Polariscope

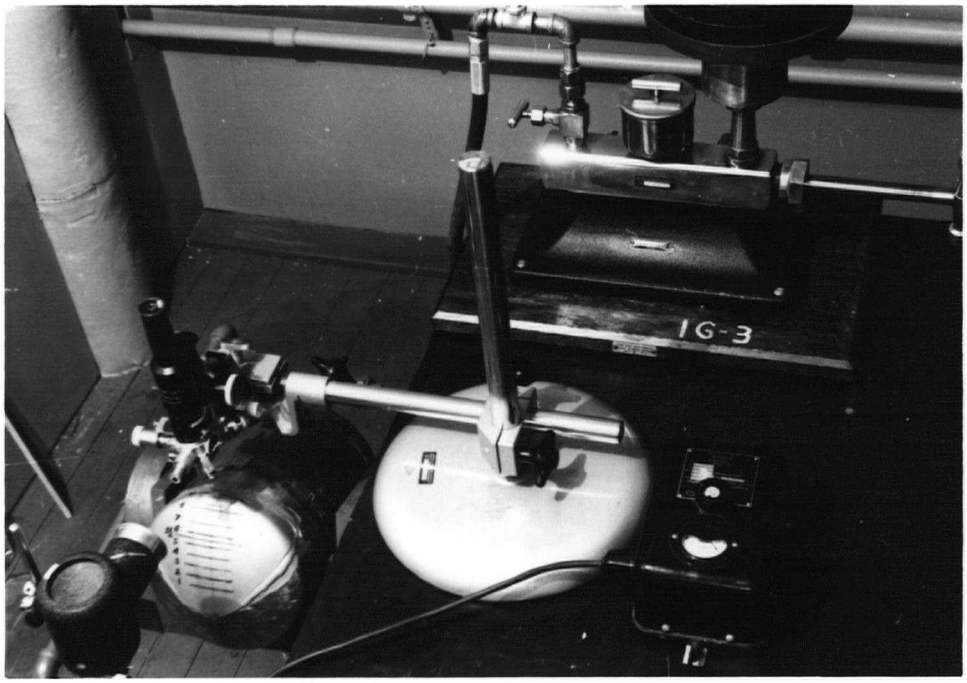

Fig.9. Test Setup for the Polarizing Microscope

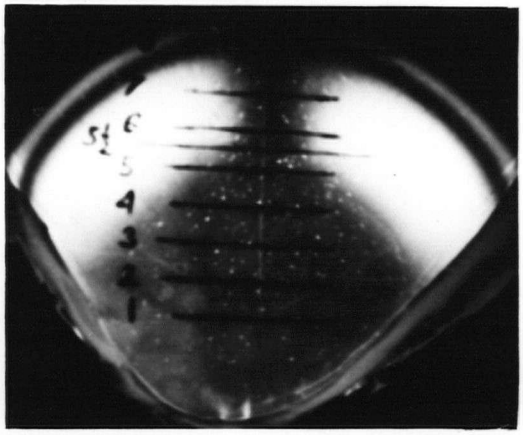

0°

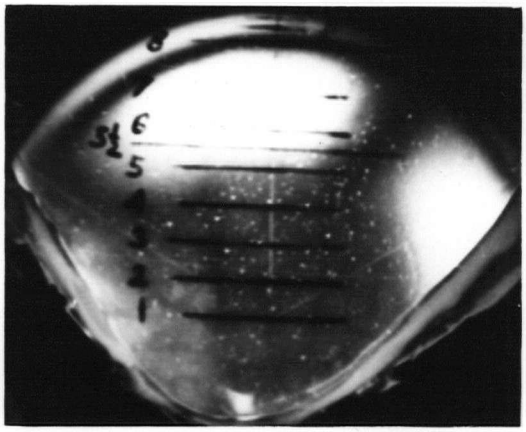

30°

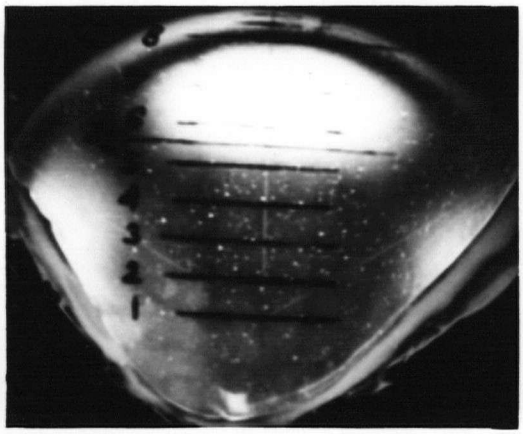

45°

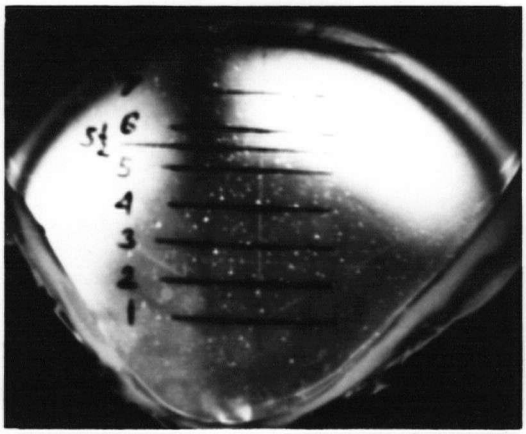

75°

Fig.10. Isoclinics on the Head of the Pressure Vessel

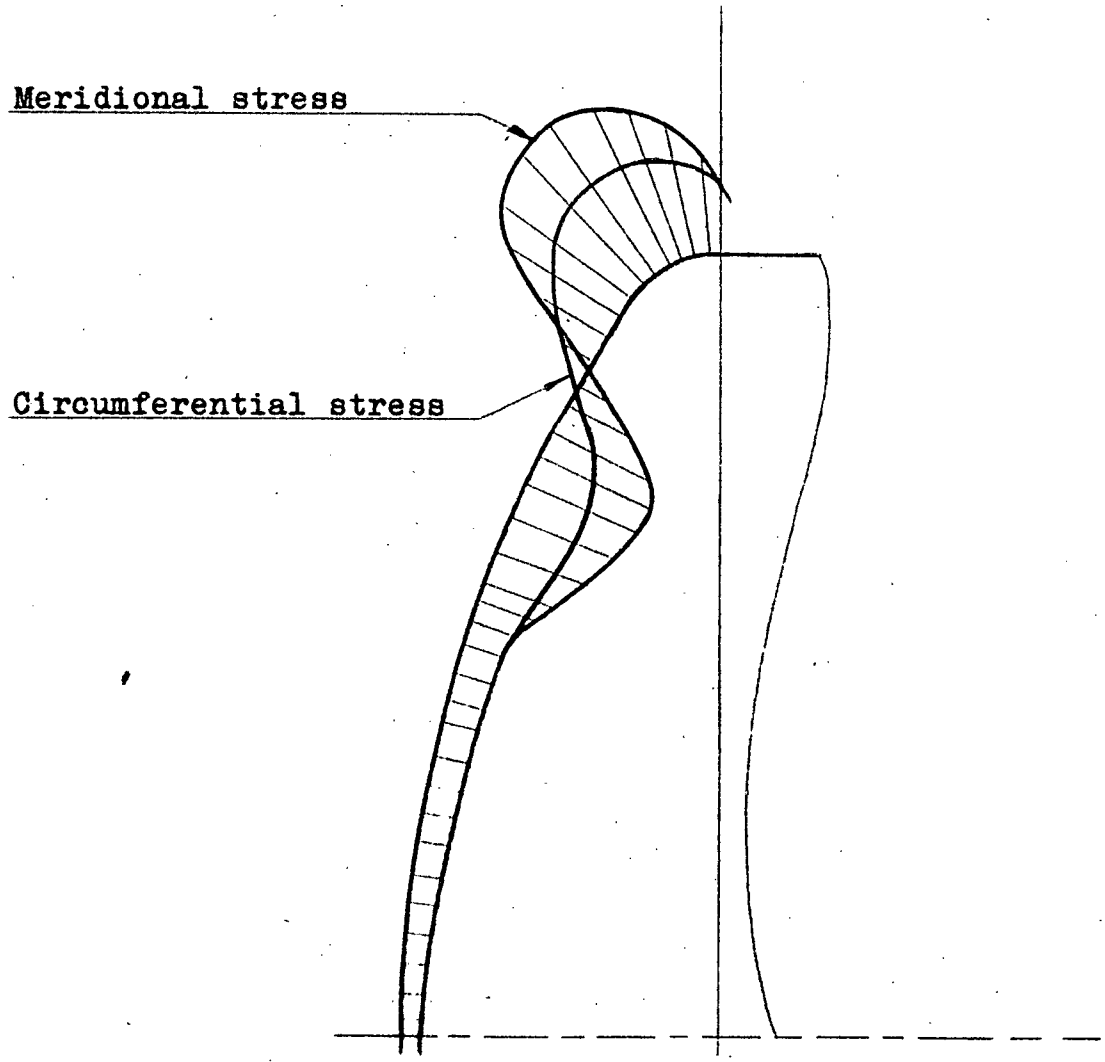

Fig.11. Stress distribution on the head of the pressure vessel

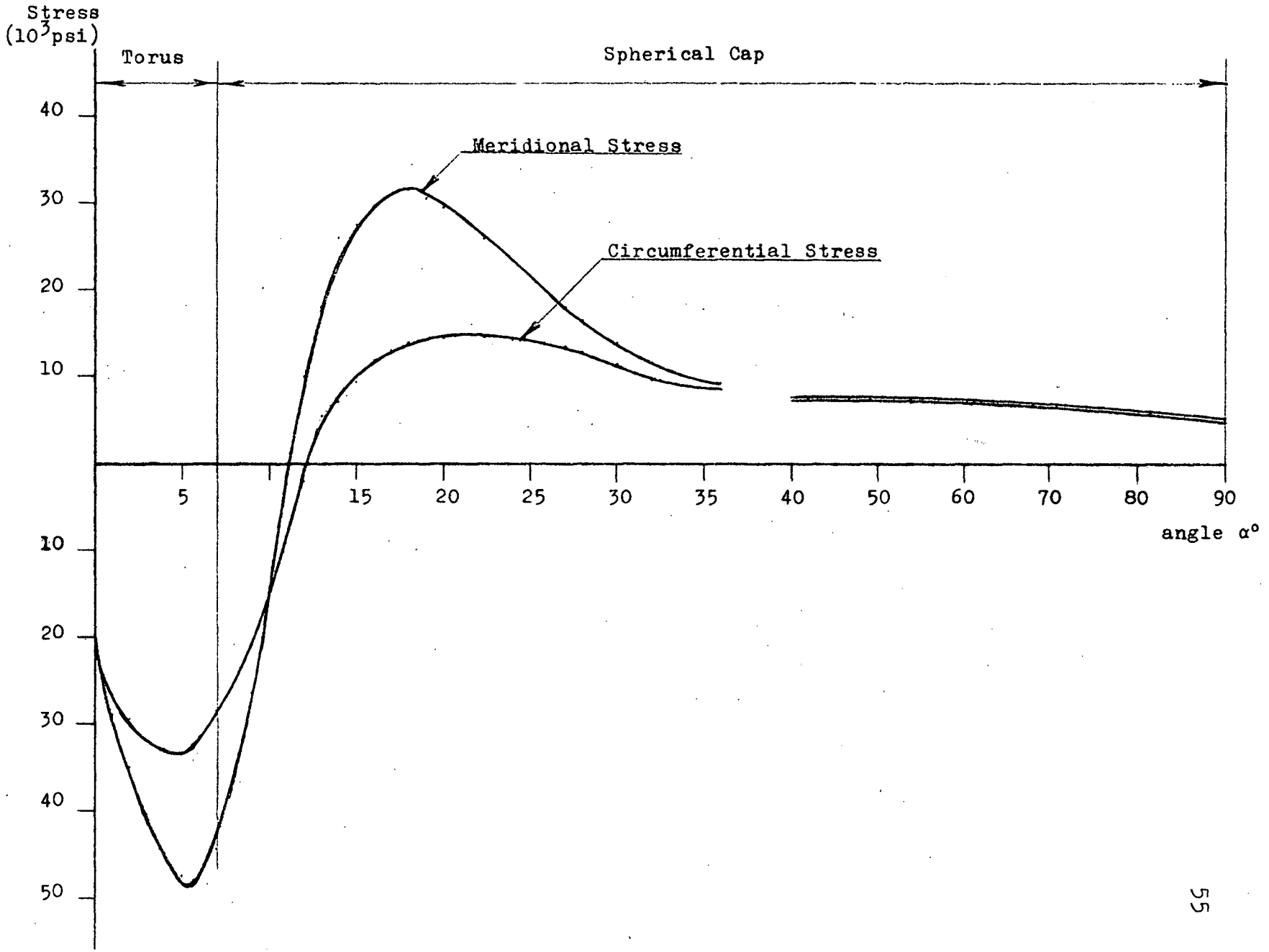

Fig. 12. Circumferential and Meridional Stresses along a radial line.

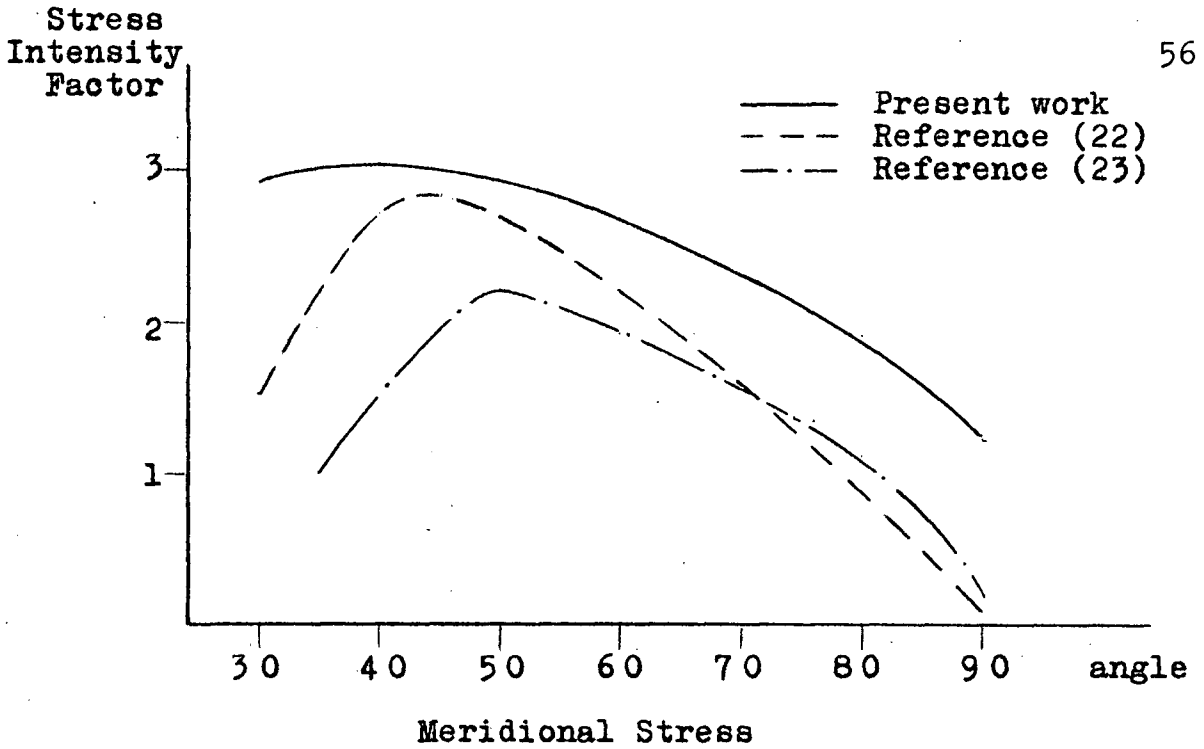

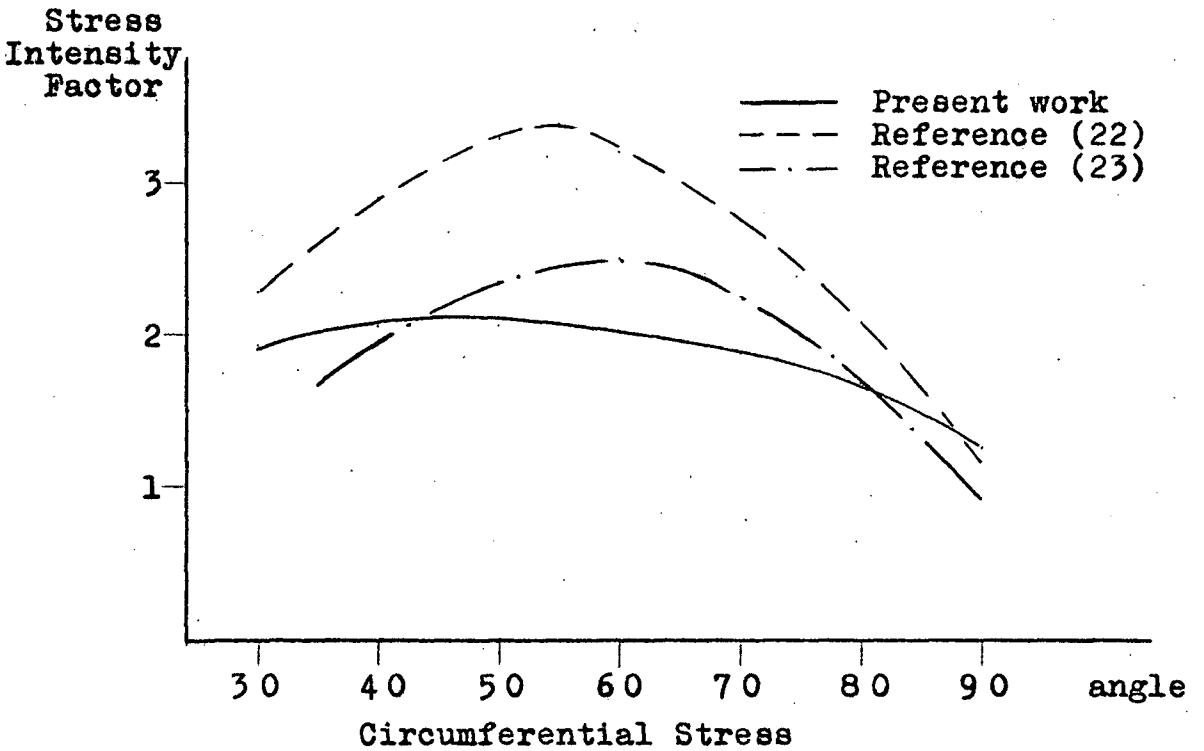

Fig.13. Stress Distribution in the Torus

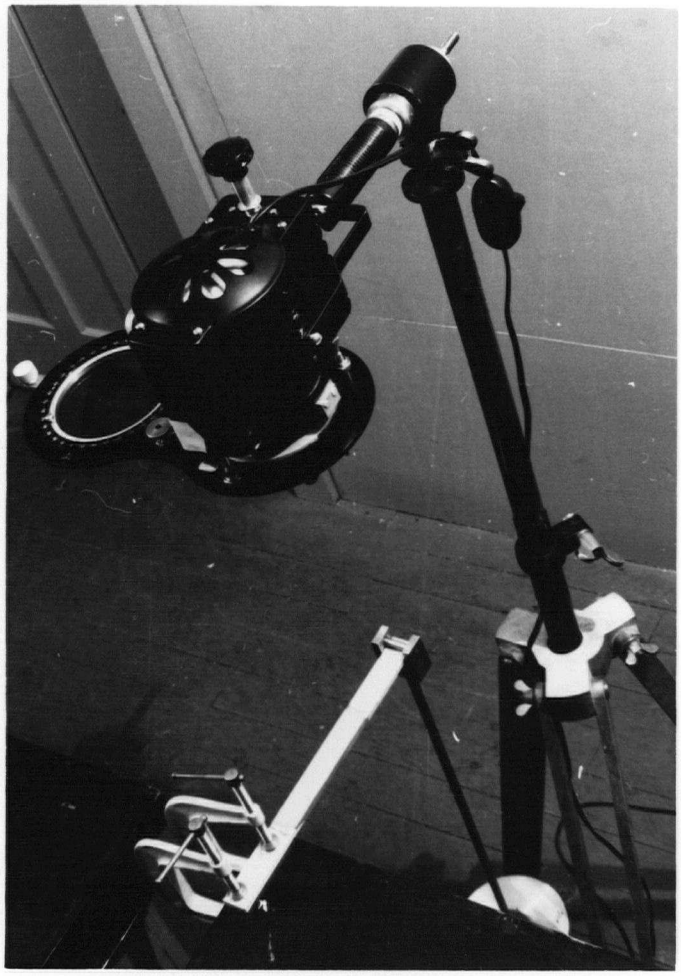

Fig.14. Test Setup for Calibration of Plastic

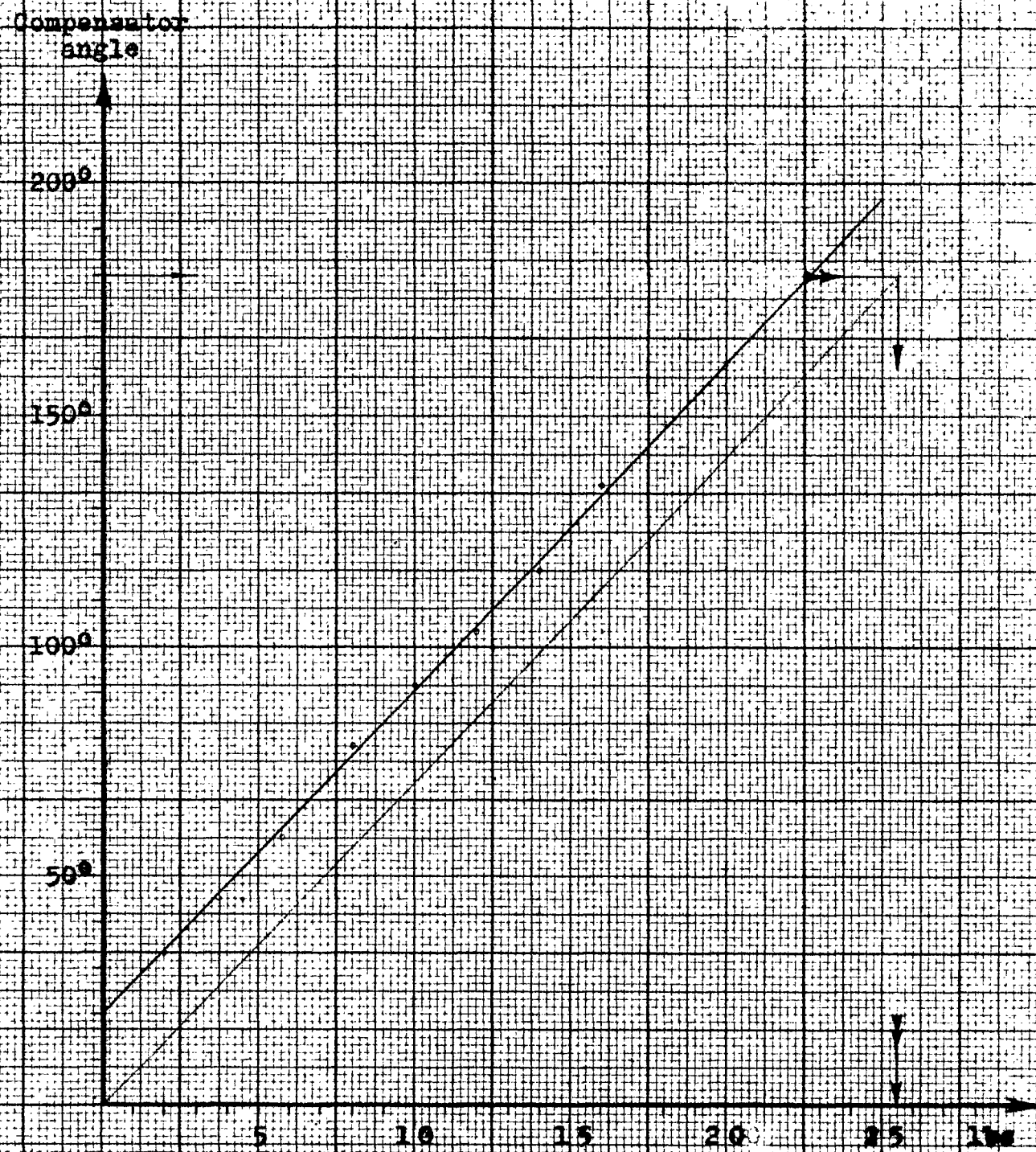

Fig.15. Calibration line of plastic